INFECTION AND IMMUNITY, Apr. 1991, p. 1489–1499
0019-9567/91/041489-11$02.00/0

Vol. 59, No. 4

# Responses of Murine Natural Killer Cells to Binding of the Fungal Target *Cryptococcus neoformans*

MICHELLE R. HIDORE, TIMOTHY W. MISLAN, AND JUNEANN W. MURPHY*
*University of Oklahoma Health Sciences Center, Oklahoma City, Oklahoma 73190*

Received 11 September 1990/Accepted 25 January 1991

**Natural killer (NK) cells bind to and inhibit the growth of the fungal target *Cryptococcus neoformans*. Since *C. neoformans* is structurally and chemically distinct from the standard tumor cell target used in the model of NK cell-mediated cytotoxicity, this study was designed to investigate the NK cell response after binding to cryptococci. Transmission electron micrographs and three-dimensional reconstructions of NK cell-cryptococci conjugates demonstrated focusing of the NK cell centrioles and Golgi apparatus toward the cryptococcal attachment site. NK cell cytoskeletal changes after cryptococcal binding were confirmed by immunofluorescence studies in which NK cells were allowed to bind to cryptococci in $Mg^{2+}$-containing, $Ca^{2+}$-free medium. One hour after the addition of $Ca^{2+}$ to the preformed conjugates, the bound NK cells demonstrated a significant increase in the percentage of microtubule organizing centers focused toward the cryptococcal binding site. Colchicine, a drug that inhibits microtubule assembly, did not affect NK cell-cryptococci binding but abrogated NK cell-mediated cryptococcal growth inhibition, indicating that microtubule assembly, an important prerequisite for the secretory process, is not required for NK cell-cryptococci binding but is essential for inhibition of cryptococcal growth. In addition, the $Ca^{2+}$ channel-blocking reagents, lidocaine and verapamil, did not affect NK cell-cryptococci binding but blocked the NK cell-mediated anticryptococcal activity, suggesting that a $Ca^{2+}$ flux is essential for inhibition of cryptococcal growth. Considered together, these data indicate that NK cells respond to binding of a target cell that has a capsule and cell wall, in addition to a cell membrane, in a manner similar to that seen following binding to target cells that are surrounded by only a cell membrane; however, the response of the NK cells to the binding of *C. neoformans* is slower and possibly less efficient than the response after tumor cell binding.**

Natural killer (NK) cells are generally considered to play an important role in innate host defense against tumor or virus-infected cells (8). We have shown that NK cells also play a role in host defense against a mycotic disease-causing agent, *Cryptococcus neoformans* (10–13, 26, 28, 29). As with the tumor cell targets, NK cells bind to the cryptococcal cells before inflicting damage to this yeastlike target cell (12, 26, 29). However, *C. neoformans* cells are structurally different from the tumor or tissue cell targets which are commonly attacked by NK cells. For instance, in contrast to the plasma membrane, the structure of the tumor cell that comes into direct contact with the NK cells, the outer surface of the cryptococcal cell is a polysaccharide capsule that covers the cell wall. The capsule and the rigid nature of the cryptococcal cell wall impede direct contact of the NK cells with the plasma membrane and prevent cryptococcal cell lysis after NK cell-mediated damage. Although tumor cell lysis is the standard measure of NK cell-mediated cytotoxicity (20), the lack of cryptococcal cell lysis precludes the use of a similar assay as a measure of NK cell-mediated damage to cryptococcal cells. Therefore, inhibition of cryptococcal growth is measured as the indicator of NK cell-mediated cryptococcal damage (28). Considering these structural differences between the cryptococcal target cell and the standard tumor cell target, our most recent studies have compared the series of events required for NK cell-mediated anticryptococcal activity with the series of events that culminate in NK cell-mediated tumor cell lysis.

NK cell-mediated tumor cell cytotoxicity has been resolved by other investigators into five stages, including (i) binding, (ii) programming of the NK cell, (iii) delivery of the lethal hit, (iv) killer cell-independent lysis, and (v) recycling (15, 16, 38). A series of cytoplasmic events, termed programming of the NK cell, follows $Mg^{2+}$-dependent binding of NK cells to susceptible tumor cell targets but does not occur after binding to nonsusceptible tumor targets. The programming stage is $Ca^{2+}$ dependent and prerequisite to the delivery of the lethal hit (15, 16, 38). In the model of NK cell-mediated tumor cell cytotoxicity, the series of events that define programming of the effector cell includes (i) microtubule assembly (19, 21); (ii) a polarized reorientation of the cytoplasmic granules (5), the Golgi apparatus (4, 21), the microtubule-organizing center (MTOC; 21), and other cytoskeletal components (2, 34) into the area of the cytoplasm adjacent to the bound target cell; and (iii) an apparent requirement for a $Ca^{2+}$ flux into the effector cell (16, 38).

Our previous studies have demonstrated both differences and similarities between NK cell-cryptococci interactions and NK cell-tumor cell interactions (12, 13). For example, there are distinct physical and kinetic differences in NK cell-cryptococci target binding and growth inhibition in comparison to NK cell binding and lysis of tumor cell targets. The time required for NK cells to bind to and inhibit the growth of cryptococci is extended in comparison to the time required for binding and lysis of tumor cell targets (26). In addition, the contact area of NK cell-cryptococci conjugates is much less intimate than that of NK cell-tumor cell conjugates (14, 26, 32). However, we have also demonstrated similarities in the temperature and divalent cation requirements for NK cell-mediated cryptococcal growth inhibition and tumor cell lysis (12). These data suggest that the physical differences between cryptococcal target cells and tumor target cells dictate, to some degree, the nature of

* Corresponding author.

the cell-cell interactions with NK cells; therefore, further studies were warranted to determine whether binding of the two distinctly different target cells triggers at least some similar NK cell responses.

The studies presented here were designed to further compare the NK cell response after binding of two distinctly different target cells, the fungus *C. neoformans* and the YAC-1 tumor cell. Through the use of transmission electron microscopy (TEM) and binding and cytotoxicity assays with cryptococcal target cells, we assessed the NK cell response, during the programming stage, that follows NK cell binding to a *C. neoformans* target cell.

## MATERIALS AND METHODS

**Mice.** Female CBA/J mice were obtained from Jackson Laboratories, Bar Harbor, Me. The animals were maintained in the University of Oklahoma (Norman and Oklahoma City) animal facilities until they were used for these studies at 8 to 10 weeks of age.

**Reagents.** EGTA [ethylene glycol-bis(β-aminoethyl ether)-N,N,N′,N′-tetraacetic acid] (2.5 mM), $MgCl_2$ (2.5 mM), $CaCl_2$ (5.0 mM), colchicine ($10^{-4}$ M), lidocaine (1 mM), and verapamil (0.2 mM) were prepared in complete medium (CM) consisting of RPMI 1640 medium (GIBCO Laboratories, Grand Island, N.Y.) supplemented with 10% heat-inactivated fetal bovine serum, 100 U of penicillin per ml, and 100 μg of streptomycin per ml. The reagent concentrations indicated were the final concentrations of each reagent within the assay samples. All reagents were purchased from Sigma Chemical Co., St. Louis, Mo.

**Fungal target.** *C. neoformans* isolate 184A was maintained on modified Sabouraud agar slants (27). After 3 days of growth at room temperature, blastoconidia were harvested, washed three times in sterile physiological saline, and adjusted to the desired cell concentration for each experiment with CM. Cell concentrations were based on hemacytometer counts and confirmed by determining the CFUs on modified Sabouraud agar plates.

**Effector cells.** Murine splenic nylon wool-nonadherent (NWN) cells were isolated as previously described (18) and used as effector cells in certain assays or further enriched for NK cells on discontinuous Percoll gradients by the method that we have previously described in detail (29). Routinely with this protocol, the anti-YAC-1 activity is significantly enriched in the cell fractions from the low-density Percoll layers (fractions 1 and 2) compared with the anti-YAC-1 activity of the input NWN cell population. Typically, the NWN spleen cell populations that we collect contain, on an average, 75% Thy-$1^+$ cells, 2 to 3% mouse $Ig^+$ cells, 1 to 2% nonspecific esterase-positive cells, 9 to 10% asialo $GM_1{}^+$ cells, and 6% large granular lymphocytes (cells with NK cell morphology and detectable granules in the cytoplasm); whereas, Percoll fraction 1 and 2 cell populations contain 20% Thy-$1^+$ cells, no mouse $Ig^+$ or nonspecific esterase-staining cells, 40% asialo $GM_1{}^+$ cells, and 36% large granular lymphocytes, with most of the remaining cells being large agranular lymphocytes (29). In a previous study, we showed with scanning electron microscopy that the Percoll fraction 1 and 2 effector cells bound to *C. neoformans* target cells were asialo $GM_1{}^+$ cells (29). For convenience throughout the remainder of this paper, we have referred to the Percoll fraction 1 and 2 cells which are highly enriched for NK cells as NK cells. NK cell fractions were adjusted to the appropriate concentration for each assay in CM and used as effector cells in these studies. Trypan blue dye exclusion ascertained that the variable reagents that were added to specific experiments did not alter effector cell viability.

***C. neoformans* growth inhibition assay.** To assess NK cell-mediated inhibition of *C. neoformans* growth, the assay previously described by Murphy and McDaniel was used (28). Briefly, $10^6$ splenic NWN cells and $2 \times 10^3$ cryptococcal target cells suspended in CM were added to quadruplicate wells of a flat-bottom, 96-well microtiter plate (Linbro Scientific Co., Hamden, N.Y.). Quadruplicate control wells contained cryptococcal target cells in CM. Both experimental and control well volumes were adjusted to 0.25 ml with CM or with an appropriate dilution of the variable reagent in CM. Cryptococcal controls containing the variable to be assayed were included to ascertain that the culture conditions alone were not inhibitory to cryptococcal growth. After incubating the plate for 18 h at 37°C in 5% $CO_2$, the content of each well was serially diluted in sterile physiological saline and plated in duplicate on modified Sabouraud agar plates. After 3 days of incubation at room temperature, CFU were enumerated and the percentage of cryptococcal growth inhibition was determined according to the following formula: % cryptococcal growth inhibition = [(mean control CFU − mean experimental CFU)/mean control CFU] × 100.

**YAC-1 cytolytic assay.** To assay the level of splenic NK cell activity, we performed a standard assay measuring the $^{51}Cr$ released from YAC-1 target cells as previously described (12, 20). Briefly, $10^6$ splenic NWN effector cells and $2 \times 10^4$ $^{51}Cr$-labeled YAC-1 tumor cells suspended in CM were added to quadruplicate wells of a 96-well, round-bottom microtiter plate. Spontaneous release samples contained YAC-1 cells in CM; whereas, maximum release samples contained YAC-1 cells in 2 N HCl. The volumes of experimental wells, spontaneous release wells, and maximum release wells were adjusted to 0.2 ml with either CM or the variable reagent to be assayed appropriately diluted in CM. After 4 h of incubation at 37°C in 5% $CO_2$, 0.1 ml of each supernatant was collected from the wells and counted in a Beckman gamma counter (Beckman Instruments, Inc., Fullerton, Calif.). Numerous studies have demonstrated that the percentage of $^{51}Cr$ released is a direct correlate of the percentage of cytotoxicity or lysis of YAC-1 target cells (20, 24). In the experiments in which the effects of a variable reagent on YAC-1 cytolysis were assessed, appropriate spontaneous release and maximum release control wells containing an equivalent concentration of the variable reagent to that used in the experimental wells were included. The percentage of $^{51}Cr$ released from YAC-1 target cells was calculated by using the following formula: % $^{51}Cr$ released = [(counts per minute of experimental supernatant − counts per minute of spontaneous supernatant)/counts per minute of maximum supernatant] × 100. The $^{51}Cr$ release assays were performed in parallel with the cryptococcal growth inhibition assays in these studies to ascertain that the various culture conditions did not adversely affect the activity of the effector cells.

**Assay for effector cell-target cell conjugate formation.** Binding of effector cells to either *C. neoformans* or YAC-1 target cells was assessed by the procedure previously described (12, 29). Briefly, effector cells, either splenic NWN cells or NK cells, were mixed with target cells at an effector-cell-to-target-cell ratio of 2:1 in CM or a designated variable reagent diluted in CM. The effector cells were incubated with the target cells for times previously determined to be optimal for maximum NK cell-target cell binding (2 h at 37°C in 5% $CO_2$ for cryptococcal target cells or 1 h with similar culture conditions for YAC-1 target cells) (26). To facilitate counting

of the NK cell-cryptococcal cell conjugates, those samples were stained with 0.25% alcian blue in serum-free RPMI 1640 medium. A sample of each conjugate suspension was counted by light microscopy, and the percentage of effector cells bound to target cells was calculated by counting a minimum of 200 effector cells.

**Cell preparation for TEM.** NK cells were mixed with *C. neoformans* target cells at an effector-cell-to-target-cell ratio of 2:1 in 0.2 ml of CM. After 12 h of incubation at 37°C in 5% $CO_2$, the cell suspension was washed with Hanks balanced salt solution (GIBCO), resuspended in 0.2 ml of RPMI 1640 medium, and placed on acetate film (Eastman Kodak Co., Rochester, N.Y.) that was precoated with 0.1% poly-L-lysine (Sigma). The cell suspension was incubated on the acetate film for 1 h at 4°C to allow the cells to adhere to the film. The cells were fixed for 30 min at 4°C with 3% glutaraldehyde (vol/vol)-6% paraformaldehyde (vol/vol)-0.2% tannic acid (wt/vol) diluted with 0.1 M sodium phosphate buffer (pH 7.4). The fixed cells were washed with three changes of 0.1 M sodium phosphate buffer at 4°C and postfixed for 30 min at 4°C with 0.1 M sodium phosphate buffer containing 1% osmium tetroxide (wt/vol) and 0.01% ruthenium red (wt/vol). Following three washes in 0.1 M sodium phosphate buffer at 4°C, the cells were dehydrated in a graded series of ethanol dilutions and infiltrated with Spurr's low viscosity resin (37). After flat-embedding, the cells were serially sectioned into 100-nm sections with a diamond knife on a Sorvall MT-6000 or a Reichart Ultracut ultramicrotome and the thin sections were collected by the method of Galey and Nilsson (6). Thin sections were mounted on Formvar- and carbon-coated copper slot grids, stained with 0.5% uranyl acetate (wt/vol) and Reynold's lead citrate (31), and examined on a Zeiss 10A electron microscope at 40 or 60 kV. The electron microscopy grade reagents and grids used to prepare the cells for TEM were purchased from Electron Microscopy Sciences, Fort Washington, Pa.

**Three-dimensional reconstructions of NK cell-*C. neoformans* conjugates.** Three-dimensional reconstructions of NK cell-cryptococci conjugates were prepared by tracing serial sections (100 nm) of each complete conjugate on a Summa Sketch Plus, which transfers the data into the IBM PC-based Three Dimensional Reconstruction System of S. M. Royer and J. C. Kinnamon, University of Colorado, Boulder.

**$Ca^{2+}$ pulse technique.** For studying the reorientation of NK cell organelles after the NK cells associate with the cryptococcal target, we allowed the effector and target cells to bind in $Mg^{2+}$-containing, $Ca^{2+}$-free conditions and then added $Ca^{2+}$ to synchronize the initiation of the postbinding events in the NK cell-*C. neoformans* conjugates. We have previously demonstrated that NK cell-cryptococci binding requires $Mg^{2+}$; whereas $Ca^{2+}$ is essential to initiate the programming stage that is prerequisite to the subsequent events which result in NK cell-mediated cryptococcal growth inhibition (12). Therefore, to achieve maximal NK cell-*C. neoformans* binding, NK cells were incubated for 2 h at 37°C with cryptococcal target cells in $Mg^{2+}$-containing, $Ca^{2+}$-free culture conditions, i.e., CM supplemented with 2.5 mM $MgCl_2$ and 2.5 mM EGTA. After the 2 h that was required for binding, $CaCl_2$ was added to the cell suspension at a final concentration of 5.0 mM to initiate the postbinding events which are prerequisite to the inhibitory event. At various times before and after the $Ca^{2+}$ addition, samples of the conjugate suspensions were collected for indirect immunofluorescence assays.

**Indirect immunofluorescence.** The orientation of the MTOC and microtubules within NK cells was assessed by an indirect immunofluorescence staining technique that labeled tubulin, the protein subunit of microtubules. Cell suspensions containing conjugates were collected at various times during the $Ca^{2+}$ pulse assay, washed two times in $Ca^{2+}$-$Mg^{2+}$-free Hanks balanced salt solution, and resuspended in 0.1 ml of the same medium. The washed cells were allowed to adhere for 1 h at 4°C to 22-mm round glass coverslips that had been precoated with 0.1% poly-L-lysine (wt/vol). After rinsing the coverslips briefly in 0.01 M phosphate-buffered saline (PBS) to remove the culture medium, the conjugates were fixed for 10 min with 4% paraformaldehyde and 0.01% ruthenium red in PBS, washed two times for 5 min with PBS, and permeablized by immersion for 10 min in acetone that was prechilled to 0°C. Following two washes with PBS, the cells were incubated with a blocking buffer of PBS supplemented with 1% bovine serum albumin (BSA) for 10 min and then washed two times with PBS containing 0.05% Tween 20 (vol/vol). After preblocking, 0.04 ml of rabbit antisea urchin tubulin (whole serum) diluted 1:25 in PBS containing 1% BSA was placed on each coverslip. Following a 45-min incubation, the conjugates were washed two times with PBS plus 0.05% Tween 20, and then each coverslip was incubated for 30 min with 0.04 ml of tetramethylrhodamine isothiocyanate (TRITC)-conjugated goat anti-rabbit immunoglobulin G $F(ab')_2$ fragments (Jackson Immunoresearch Laboratories, Avondale, Pa.) diluted 1:50 in PBS plus 1% BSA. The fluorochrome-labeled cells were washed two times with PBS with 0.05% Tween 20 and once with distilled water before inverting the coverslips into a drop of Fluoromount-G (Southern Biotechnology Associates, Birmingham, Ala.) on a glass microscope slide. Conjugates were examined with an Olympus BH-2 microscope equipped with phase-contrast optics, epifluorescence illumination, and rhodamine fluorescence optics (Olympus Corp., Lake Success, N.Y.). Effector cells bound to cryptococcal target cells were considered to have a positively focused MTOC if the MTOC was located in either of the two quadrants of the effector cell cytoplasm adjacent to the bound target cell. A minimum of 300 NK cells were scored for the presence or absence of tubulin networks or for positive or negative focus of the MTOC in relation to the bound cryptococcal target cell.

**Statistical analysis.** Means and standard errors of the means were calculated, and the two-tailed Student's *t* test was used to analyze the data.

## RESULTS

**Organization of the NK cell cytoplasm after binding to a *C. neoformans* target cell.** Initial studies employed TEM to assess the orientation of the cytoplasmic organelles within NK cells in relation to the binding site of the cryptococcal target cell. After incubating the NK cells with *C. neoformans* target cells for 12 h, NK cell-cryptococci conjugates were fixed for TEM and serially sectioned. Figure 1 shows TEMs of one of the 100-nm sections of a representative NK cell-cryptococci conjugate. The nucleus of the NK cell was located away from the cryptococcal binding site, whereas the Golgi apparatus, mitochondria, and centrioles were focused in the area of the NK cell cytoplasm adjacent to the cryptococcal binding site (Fig. 1). A computer-generated three-dimensional reconstruction of this same NK cell-cryptococci conjugate, prepared from electron micrographs of the complete series of 100-nm sections of the entire conjugate, is shown in Fig. 2a. The three-dimensional method of viewing this conjugate reiterates the polarized

a
NK cell
nucleus
Golgi apparatus
centrioles
C. neoformans cell
capsule
cell wall
b
Golgi apparatus
centrioles

FIG. 1. TEMs of a 100-nm section through an NK cell-*C. neoformans* conjugate. Percoll fractionated splenic large granular lymphocytes were incubated with cryptococcal target cells for 12 h before preparation for TEM. A higher magnification of the Golgi apparatus is shown in panel b. Bars, 1 μm.

orientation of the organelles within the effector cell cytoplasm in relation to the cryptococcal attachment site. The Golgi apparatus and centrioles are focused in the area of the effector cell cytoplasm adjacent to the cryptococcal target cell, whereas the nucleus of the NK cell is opposite to the target cell attachment site (Fig. 2a). A three-dimensional reconstruction of a second representative NK cell-cryptococci conjugate, which also demonstrates focusing of the NK cell Golgi apparatus and centrioles toward the cryptococcal binding site, is shown in Fig. 2b. The polarized orientation of the NK cell's Golgi apparatus and centrioles toward the attachment site of the cryptococcal target cell was a frequent observation both in the individual thin sections and in the reconstructions of the NK cell-cryptococci conjugates. Therefore, further studies were designed to assess the relationship of this polarized reorientation of the effector cell organelles to the time of cryptococcal binding and to the onset of the $Ca^{2+}$-dependent postbinding stage of NK cell-mediated cryptococcal growth inhibition.

**Tubulin distribution within NK cells during the $Ca^{2+}$ pulse assay.** To determine the onset of the NK cell cytoplasmic reorganization in relation to the sequence of binding and inhibition of the cryptococcal target cell, the distribution of tubulin within the NK cell was determined by indirect immunofluorescence at various times following the addition of $Ca^{2+}$ to the NK cell-cryptococci mixtures. We have

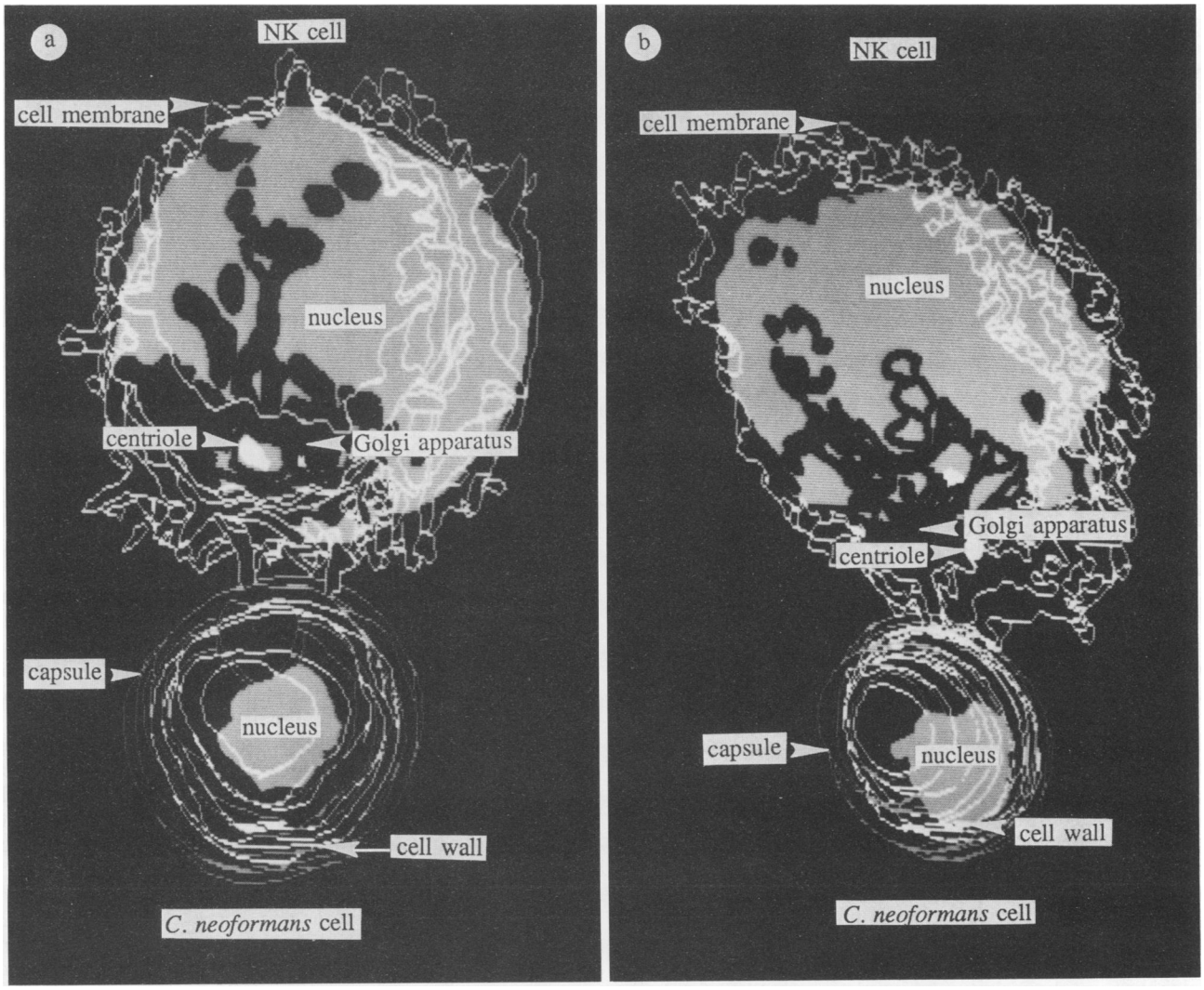


FIG. 2. Three-dimensional reconstructions of two different NK cell-*C. neoformans* conjugates (a and b) prepared from electron micrographs of 100-nm serial sections of each complete conjugate. Percoll-fractionated splenic large granular lymphocytes were incubated with cryptococcal target cells for 12 h before preparation for TEM. The NK cell structures shown are the plasma membrane (outlined white), nucleus (solid grey), centrioles (solid white), and Golgi apparatus (solid black). The *C. neoformans* structures shown are the capsule (outlined grey), cell wall (outlined white), and nucleus (solid grey).

previously demonstrated that NK cell-cryptococci binding requires $Mg^{2+}$, whereas the subsequent stages that result in the growth-inhibitory event only proceed after $Ca^{2+}$ is added to the $Mg^{2+}$-containing conjugates (12). Therefore, NK cells were allowed to bind to cryptococci in $Mg^{2+}$-containing culture conditions for 2 h, a time previously determined to promote maximal NK cell-cryptococci conjugate formation (26), and then $Ca^{2+}$ was added to initiate the subsequent stages that result in cryptococcal growth inhibition. At various times before and after the addition of $Ca^{2+}$, microtubule assembly and the orientation of the MTOC within the NK cells was assessed by indirect immunofluorescence labeling of tubulin, the protein subunit of microtubules. NK cells alone and NK cells conjugated to cryptococcal target cells were assessed for labeling of the MTOC and assembled microtubules (Fig. 3D to F). NK cells bound to cryptococci were not considered to be focused if the MTOC was located in either of the two quadrants of the NK cell cytoplasm opposite to the target binding site (Fig. 3D), whereas the NK cells were considered to be positively focused if the fluorescently labeled MTOC was located in the two quadrants adjacent to the cryptococcal binding site (Fig. 3E and F).

The percentage of unbound effector cells which exhibited detectable organized microtubule networks increased throughout the 4-h assay (Fig. 4a). This increase in the percentage of unbound effector cells displaying MTOCs and microtubule networks was most dramatic 30 min after the addition of $Ca^{2+}$ (Fig. 4a). A similar pattern of tubulin-positive effector cells was also observed in the unbound effector cells when the NK cell-cryptococci mixtures were incubated in $Ca^{2+}$-$Mg^{2+}$-free medium for 4 h or when effector cells alone were incubated by using the conditions of adding $Ca^{2+}$ at 2 h to $Mg^{2+}$-containing medium (data not shown). In addition, the changes in the percentage of tubulin-positive effector cells that were conjugated to cryptococcal target cells (Fig. 4b) were similar to those observed for the unbound effector cells (Fig. 4a).

In the effector cells bound to cryptococcal target cells, enumeration of the positively focused MTOC revealed a random distribution (50%) of effector cell MTOCs in conjugates formed in $Mg^{2+}$-containing, $Ca^{2+}$-free medium (2 h) or in $Mg^{2+}$-containing medium 30 min after the addition of $Ca^{2+}$ (2.5 h) (50% ± 5% and 52% ± 2%, respectively; Fig. 4c). In contrast, 1 h after initiation of the $Ca^{2+}$-dependent programming stage by the addition of $Ca^{2+}$ to the $Mg^{2+}$-containing conjugates (3 h), there was a significant increase ($P < 0.01$, when compared with the results at the 1-, 2-, 2.5-, or 4-h times) in the percentage of NK cells with the MTOC positively focused toward the cryptococcal target cell (Fig. 4c). By 2 h after initiation of the programming stage (4 h into the assay), a random distribution of the MTOCs within effector cells bound to cryptococci was again observed (Fig. 4c).

**Effects of colchicine on NK cell binding and inhibition of *C. neoformans*.** The previous experiments indicated that NK cell cytoskeletal changes, as assessed by reorientation of the MTOC within the NK cells, occurred within 1 h after the initiation of the $Ca^{2+}$-dependent events that result in NK cell-mediated cryptococcal growth inhibition. Therefore, the requirement for microtubule assembly during NK cell binding and inhibition of cryptococcal growth was assessed. Colchicine, a drug that inhibits the assembly of tubulin subunits into microtubules (19, 32), was added to the NK cell-binding assay, with either cryptococci or YAC-1 target cells, and to the cryptococcal growth inhibition and $^{51}Cr$ release assays. Binding of NK cells, to either *C. neoformans* or YAC-1 target cells, was equivalent in the respective target cell samples incubated with and without colchicine (Fig. 5). In contrast, when cryptococcal growth inhibition or $^{51}Cr$ release from YAC-1 target cells was assessed, the same concentration of colchicine that allowed conjugates to form completely abrogated both of these NK cell-mediated activities (Fig. 5).

**Effects of $Ca^{2+}$ channel-blocking reagents on NK cell-mediated binding and inhibition of *C. neoformans*.** Although in previous studies we have demonstrated that extracellular $Ca^{2+}$ is required for postbinding steps that lead to inhibition of cryptococcal growth (12), it is not known whether a $Ca^{2+}$ flux into the effector cells is essential for cryptococcal growth inhibition. Therefore, to acquire preliminary information on the $Ca^{2+}$ flux requirement, lidocaine and verapamil, drugs which block $Ca^{2+}$ channels in the plasma membrane and thus prevent a $Ca^{2+}$ influx (16, 25), were added to the NK cell-binding assay with cryptococci and to the cryptococcal growth inhibition assay. Parallel studies were performed with YAC-1 target cells. NK cell conjugate formation with either cryptococci or YAC-1 target cells was equivalent in the respective target cell samples incubated with or without lidocaine or verapamil (Fig. 6). In contrast, both NK cell-mediated cryptococcal growth inhibition and $^{51}Cr$ release from YAC-1 target cells were significantly reduced from control levels in the samples containing either lidocaine or verapamil (Fig. 6).

## DISCUSSION

We have previously established that NK cells bind to and inhibit the growth of the fungus *C. neoformans* and that the growth-inhibitory activity correlates with tumoricidal activity (10–13, 26, 28, 29). The investigations reported here were designed to determine whether binding of a target cell, such as a cryptococcal cell that is structurally and chemically distinct from the classical tumor cell target, triggers a series of intracellular events within the NK cell similar to those events that occur following attachment of the tumor cell target to the NK cell.

In the model of NK cell-mediated tumor cell cytotoxicity, the effector cell-target cell interactions have been divided into five sequential stages (15, 16, 38). Programming of the NK cell for delivery of the lethal hit, the second stage, is defined by a series of $Ca^{2+}$-dependent intracellular events that follow binding of the NK cell to the tumor cell target and are prerequisite to delivery of the lethal hit (15, 16, 38). During the programming stage, the NK cell responds to tumor target cell attachment with a polarized reorientation of the NK cell Golgi apparatus and MTOC toward the attachment site of the tumor target cell, which is considered to be necessary to direct secretory components toward the target cell (2, 4, 21). In addition, there are requirements for intact microtubules, for extracellular $Ca^{2+}$, and for a $Ca^{2+}$ flux across the NK cell plasma membrane (15, 16, 38). Before the present investigation, it was not known whether NK cell binding to the fungal target, *C. neoformans*, signalled intracellular changes within the effector cell.

Our initial observations, as represented by the TEM micrographs of individual sections through NK cell-cryptococcal cell conjugates (Fig. 1) and three-dimensional reconstructions of complete NK cell-*C. neoformans* conjugates (Fig. 2), showed that a polarized orientation of the NK cell Golgi apparatus and centrioles toward the site of cryptococcal attachment occurred in the majority of conjugates. In addition, in the same conjugates, the nuclei of the NK cells

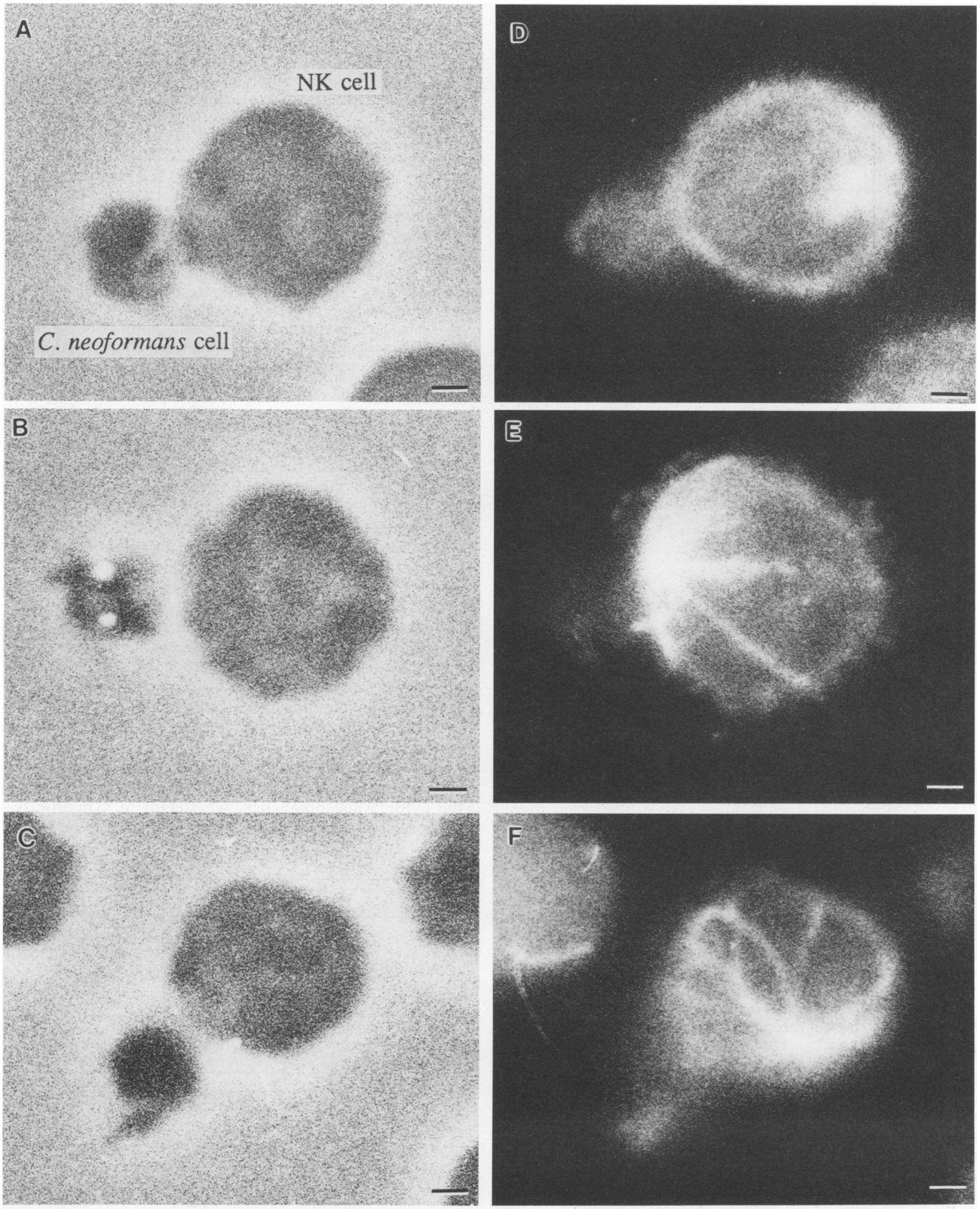


FIG. 3. NK cell-*C. neoformans* conjugates viewed with phase-contrast optics (A to C) and the corresponding conjugates (D to F, respectively) viewed with rhodamine fluorescence optics. The MTOC and microtubules of the NK cell were labeled by indirect immunofluorescence staining of tubulin and were assessed for negative (D) or positive (E and F) focusing in relation to the cryptococcal binding site. Bars, 1 μm.

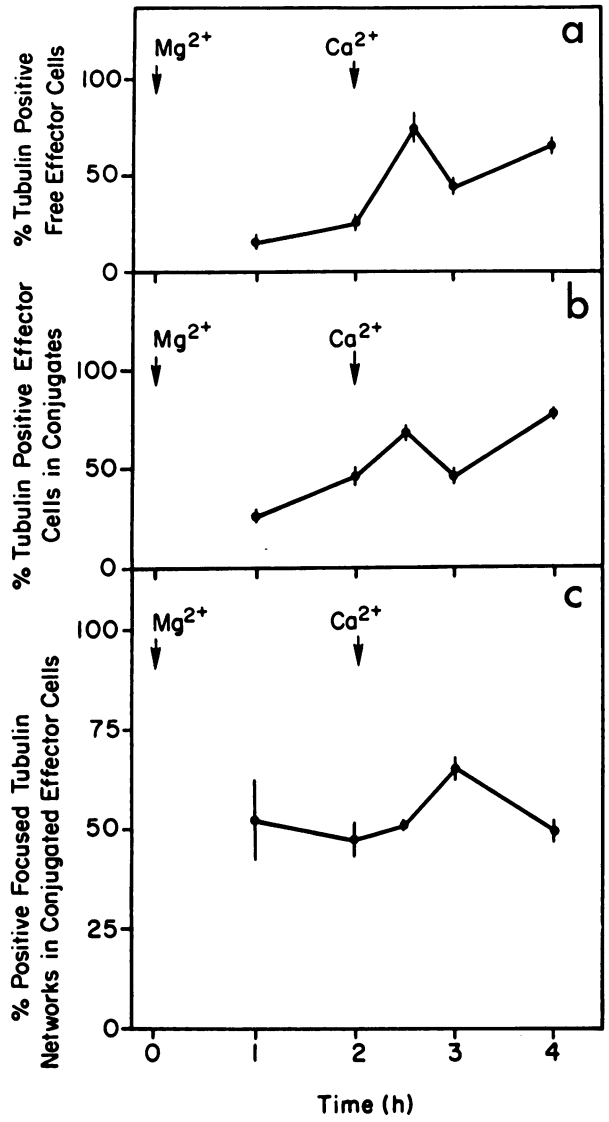


FIG. 4. Distribution of tubulin within NK cells during a $Ca^{2+}$ pulse assay. Percoll-fractionated splenic large granular lymphocytes were incubated with cryptococcal target cells in CM supplemented with 2.5 mM $MgCl_2$ and 2.5 mM EGTA for 2 h followed by the addition of 5.0 mM $CaCl_2$. NK cells alone (a) and NK cells bound to cryptococcal target cells (b) were assessed for MTOC and microtubule staining, or NK cell-cryptococcal conjugates were assessed for positive focusing of the MTOC within the NK cell toward the cryptococcal attachment site (c) by indirect immunofluorescence staining of tubulin. Data are representative of four experiments. Bars, Means ± the standard errors of the means of quadruplicate samples.

were located opposite the cryptococcal binding site (Fig. 1 and 2). Similar focusing of the effector cell Golgi apparatus and MTOC occurs following binding of NK cells and cytotoxic T lymphocytes to susceptible target cells, however nonsusceptible target cells do not trigger focusing (4, 7, 21–23). In our initial experiments, the effector and target cell mixture was incubated in complete medium for 12 h before preparing the cells for electron microscopy. By using these conditions, one would expect the time of binding of individual NK cells to cryptococcal target cells to vary and thus the

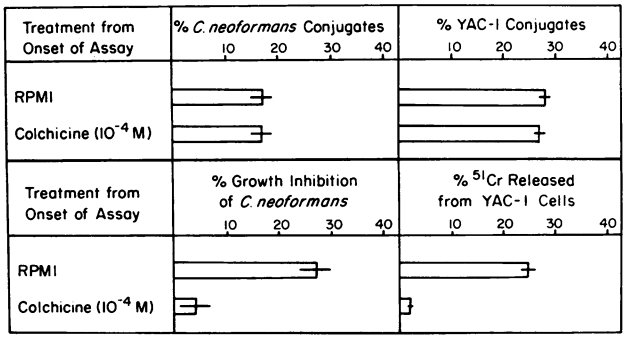


FIG. 5. Effects of colchicine on NK cell-*C. neoformans* interactions. Murine splenic NWN cells were used as effector cells in the NK cell-target cell binding assays, the cryptococcal growth inhibition assay, and the $^{51}Cr$ release assay in either CM or CM plus $10^{-4}$ M colchicine. Bars, Means ± the standard errors of the means of quadruplicate samples. Data are representative of three experiments.

initiation of the programming stage, if it occurs, to be asynchronous among various conjugates. Furthermore, if individual NK cells recycle to damage numerous cryptococcal targets, as is the case in the NK cell-tumor cell model (19, 39), then at any one time during the incubation, the individual conjugates could be at different stages in the cycle of events leading to target cell damage. Despite the fact that the conjugates observed by electron microscopy theoretically should have been at various stages of interaction, an unfocused NK cell was observed in only one of every six conjugates. Since the number of focused NK cells in conjugate formation with cryptococci was higher than expected, it appeared that binding of the cryptococcal cell to the NK cell stimulated rearrangement of the NK cell organelles. However, to validate this point, additional experiments were performed to quantify the number of focused NK cells bound to cryptococci.

For a more definitive method of determining whether NK cells responded to cryptococci binding with reorientation of the cytoplasmic organelles, we sought to synchronize the onset of reorientation of the MTOC toward the target cell in

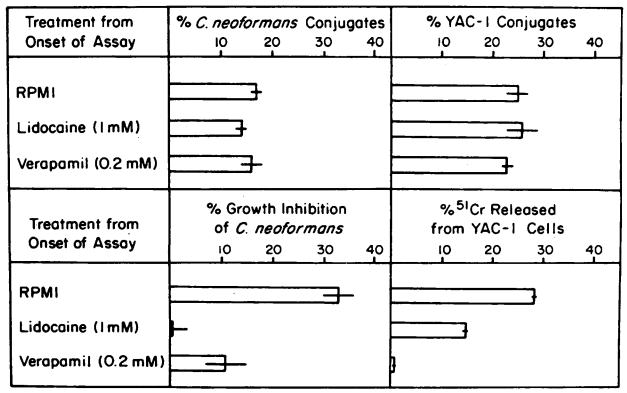


FIG. 6. Effects of lidocaine and verapamil on NK cell-*C. neoformans* interactions. Murine splenic NWN cells were used as effector cells in the NK cell-target cell binding assays, the cryptococcal growth inhibition assay, and the $^{51}Cr$ release assay in either CM, CM containing 1 mM lidocaine, or CM with 0.2 mM verapamil. Bars, Means ± the standard errors of the means of quadruplicate samples. Data are representative of three experiments.

NK cell-*C. neoformans* mixtures. Since previous studies have shown that NK cell-cryptococcal binding occurs in $Mg^{2+}$-containing, $Ca^{2+}$-free medium and that the addition of $Ca^{2+}$ is necessary to achieve NK cell-mediated inhibition of cryptococcal growth, the addition of $Ca^{2+}$ to NK cell-*C. neoformans* conjugates formed in $Mg^{2+}$-containing, $Ca^{2+}$-free medium was used in these studies to synchronize the $Ca^{2+}$-dependent postbinding events and thus to synchronize the MTOC reorientation process as well.

To gain a complete understanding of the status of the MTOC and microtubule assembly in the NK cell populations used in these studies, both the percentage of tubulin-positive (cells containing an MTOC or an MTOC and microtubule network), unbound effector cells in NK cell-cryptococci mixtures (Fig. 4a) and the percentage of tubulin-positive effector cells bound to cryptococci (Fig. 4b) were determined at designated times during the assay. Additionally, the percentage of tubulin-positive cells in NK cell populations incubated alone in the same culture conditions used for the NK cell-cryptococci mixtures and the percentage of tubulin-positive, unbound NK cells in mixtures of NK cells and cryptococci cultured in $Mg^{2+}$-containing, $Ca^{2+}$-free medium were enumerated. In all four of these situations, there were similar changes in the percentages of MTOCs and microtubule networks in the effector cells during the 4 h. These data indicate that as the NK cells are cultured in vitro over a 4-h period, increasing numbers of NK cells display MTOCs. Furthermore, in all of the situations studied, there was an increase in the percentage of tubulin-positive cells up to 2.5 h into the incubation period, and then at 3 h there was a decrease in the percentage of tubulin-positive cells compared with the percentage of tubulin-positive cells observed at 2.5 h. The decrease between 2.5 and 3 h was followed by an increase in the percentage of tubulin-positive cells over the fourth hour of the study. Since similar patterns of changes in tubulin-positive cells were observed under all conditions studied, the fluctuations in the percentage of tubulin-positive effector cells observed between 2 and 4 h were not considered to be due to the addition of $Ca^{2+}$ to the cultures. Furthermore, the data indicate that the presence or absence of cryptococci had no influence on the percentage of tubulin-positive effector cells. The findings that the unbound effector cells displayed MTOCs and tubulin networks were not unexpected when one considers that freshly isolated, unstimulated and concanavalin A-stimulated lymphocytes (1, 33) as well as human NK cells (35) have been shown to exhibit MTOCs and tubulin arrays.

When the percentage of positively focused MTOCs in NK cells conjugated to cryptococcal target cells was determined at 1, 2, 2.5, and 4 h, a random distribution (approximately 50%) of MTOCs within conjugated NK cells was observed. In contrast, 1 h after the addition of $Ca^{2+}$ (3 h into the assay) to the NK cell-*C. neoformans* mixtures, there was a significant increase in the percentage of NK cells with MTOCs located adjacent to the cryptococcal attachment site (Fig. 4c). Taken together, our data indicate that NK cells have tubulin arrays irrespective of binding to cryptococcal target cells. Furthermore, the MTOCs do not focus toward the target cells in conjugates formed in $Mg^{2+}$-containing, $Ca^{2+}$-free medium until initiation of the subsequent $Ca^{2+}$-dependent stages of NK cell-cryptococci interactions. The redistribution of the MTOCs toward the bound target cells in the conjugated effector cells requires extracellular $Ca^{2+}$ and occurs within approximately 1 h. By 2 h after the addition of $Ca^{2+}$ to the preformed NK cell-cryptococci conjugates, a random distribution of the MTOCs within the bound effector cells was again observed. This loss of focus of the MTOCs might be expected if the NK cells are in the process of recycling to another cryptococcal target cell within the hour immediately following maximum focusing of the effector cell MTOC. Kupfer et al. (22) have demonstrated that the MTOCs within approximately 95% of the effector cells bound to susceptible tumor target cells became oriented toward the target cell-binding site within 5 min after the addition of $Ca^{2+}$ to $Mg^{2+}$-containing NK cell-tumor cell conjugates and cytotoxic T lymphocyte-tumor cell conjugates. In contrast to the data of Kupfer et al. (22), a maximum of only 70% of the MTOCs within the NK cells reoriented toward the bound cryptococcal target cells, and this polarization occurred within 1 h after the addition of $Ca^{2+}$ to NK cell-*C. neoformans* conjugates in $Mg^{2+}$-containing medium (Fig. 4c). The extended time required for polarization of the MTOC toward a bound cryptococcal target cell in comparison to that required for polarization of the MTOC toward a bound tumor cell target correlated with our previous data, demonstrating that the time required for NK cells to bind to and inhibit the growth of cryptococci is extended in comparison with the time required for NK cells to bind to and mediate tumor cell lysis (26). In addition, we have previously demonstrated that the time that $Ca^{2+}$ must be present during the postbinding stages of NK cell-mediated cryptococcal growth inhibition (3 h) is also extended in comparison with the time that $Ca^{2+}$ must be present during the postbinding stages of NK cell-mediated tumor cell lysis (1 h) (12). These data demonstrate that the transmission of intercellular signals that results in the programming of the NK cell may be slower and/or less efficient after the binding of cryptococcal target cells than that which follows binding of tumor cell targets.

Redistribution of the MTOC within 1 h after the addition of $Ca^{2+}$ to the NK cell-cryptococci conjugates suggested that microtubules within the NK cell may play a role in NK cell-mediated anticryptococcal activity. Therefore, colchicine, a drug which prevents microtubule assembly (3, 19, 32), was used to determine whether inhibition of microtubule assembly affected NK cell-mediated anticryptococcal activity. Although NK cell binding to both *C. neoformans* and YAC-1 tumor cells was unaffected by colchicine, colchicine completely abrogated both NK cell-mediated cryptococcal growth inhibition and NK cell-mediated tumor cell lysis, indicating that microtubule assembly is required for NK cells to mediate anticryptococcal activity but is not necessary for NK cell-cryptococci binding (Fig. 5). NK cell-*C. neoformans* interactions are similar to those published by Roder et al. (32) for the murine model of NK cell-mediated tumor cell cytotoxicity in that intact microtubules were required for NK cell-mediated tumor cell lysis but not for NK cell-tumor cell binding.

Our observations that the binding of cryptococci to NK cells in the presence of $Ca^{2+}$ induces movement of the NK cell MTOC, and presumably the Golgi apparatus, into the region of the bound target cell is consistent with the concept that secretion is essential to NK cell-mediated cytotoxicity (8, 9, 30). Kupfer et al. (22) have suggested that reorientation of the Golgi apparatus and MTOC within NK cells bound to susceptible tumor cell targets directs Golgi apparatus-derived secretory vesicles to the site of tumor target cell contact. One could hypothesize that similar secretory processes are essential to NK cell-mediated inhibition of cryptococcal growth. The data presented here indicating that reorientation of NK cell cytoplasmic organelles occurs after binding to cryptococci and our previously published data

(13) showing that monensin, a drug that interrupts the movement of Golgi apparatus-derived vesicles to the cell membrane, blocks NK cell-mediated inhibition of cryptococcal growth lend support to this hypothesis.

Others have shown that reagents which block $Ca^{2+}$ channels in the NK cell plasma membrane abrogate tumor target cell lysis, suggesting that a $Ca^{2+}$ flux into the effector cell is required for NK cell-mediated tumor cell cytotoxicity (16, 17, 36). Our data show that the $Ca^{2+}$ channel-blocking drugs lidocaine and verapamil significantly reduced NK cell-mediated cryptococcal growth inhibition without affecting NK cell-cryptococci conjugate formation (Fig. 6). On the basis of these results, it appears that, similar to NK cell-mediated tumor cell cytotoxicity, a $Ca^{2+}$ flux across the NK cell plasma membrane at a postbinding stage is required for NK cells to mediate anticryptococcal activity.

In conclusion, our results indicate that a series of programming events follow NK cell-cryptococci binding. These events include (i) a $Ca^{2+}$-dependent, polarized reorientation of the NK cell's Golgi apparatus and MTOC toward the bound *C. neoformans* cell, (ii) microtubule assembly, and (iii) a $Ca^{2+}$ flux across the NK cell plasma membrane. The NK cell response which follows binding of the cryptococcal target cell is similar to that which occurs during programming of NK cells for tumor cell lysis, however the time required after attachment for the cryptococcal target cells to initiate the $Ca^{2+}$-dependent reorientation of NK cell organelles appears to be extended in comparison with the time required for the tumor target cells to elicit similar programming events after binding. In accordance with our previous studies demonstrating that blocking NK cell secretion of Golgi apparatus-derived vesicles abrogates cryptococcal growth inhibition and that secretory components of NK cells inhibit cryptococcal growth, reorientation of the cytoplasmic organelles and a requirement for intact microtubules suggest that the secretory process does play a role in NK cell-mediated anticryptococcal activity (13). Therefore, binding to a fungal target cell, *C. neoformans*, which is structurally and chemically distinct from the standard tumor cell target used in the model of NK cell-mediated cytotoxicity, elicits an NK cell response that is physiologically similar to, but slower and less efficient than, the response seen following NK cell binding to a tumor cell target.

## ACKNOWLEDGMENTS

This work was supported by a Public Health Service grant AI-18895 from the National Institute of Allergy and Infectious Diseases.

The electron microscopy was performed at the Samuel Roberts Noble Electron Microscopy Laboratory, Norman, Okla. The assistance of Diane Hurd and Natalie Hoshaw in preparation of the electron micrographs and three-dimensional reconstructions is greatly appreciated.

## REFERENCES

1. **Brown, D. L., K. R. Reuhl, S. Bormann, and J. E. Little.** 1988. Effects of methyl mercury on the microtubule system of mouse lymphocytes. Toxicol. Appl. Pharmacol. **94**:66–75.
2. **Carpen, O., I. Virtanen, V. Lehto, and E. Saksela.** 1983. Polarization of NK cell cytoskeleton upon conjugation with sensitive target cells. J. Immunol. **131**:2695–2698.
3. **Carpen, O., I. Virtanen, and E. Saksela.** 1981. The cytotoxic activity of human natural killer cells requires an intact secretory apparatus. Cell. Immunol. **58**:97–106.
4. **Carpen, O., I. Virtanen, and E. Saksela.** 1982. Ultrastructure of human natural killer cells: nature of the cytolytic contacts in relation to cellular secretion. J. Immunol. **128**:2691–2697.
5. **Dennert, G., A. Kupfer, C. G. Anderson, and S. J. Singer.** 1985. Reorientation of the Golgi apparatus and the microtubule-organizing center: is it a means to polarize cell-mediated cytotoxicity? Adv. Exp. Med. Biol. **184**:83–93.
6. **Galey, F. R., and S. E. G. Nilsson.** 1966. A new method for transferring sections from the liquid surface of a trough through staining solutions to the supporting film of a grid. J. Ultrastruct. Res. **14**:405–410.
7. **Geiger, B., D. Rosen, and G. Berke.** 1982. Spatial relationships of microtubule-organizing centers and the contact area of cytotoxic T lymphocytes and target cells. J. Cell Biol. **95**:137–143.
8. **Herberman, R. B.** 1986. Natural killer cells. Annu. Rev. Med. **37**:347–352.
9. **Herberman, R. B., C. W. Reynolds, and J. R. Ortaldo.** 1986. Mechanism of cytotoxicity by natural killer (NK) cells. Annu. Rev. Immunol. **4**:651–680.
10. **Hidore, M. R., and J. W. Murphy.** 1986. Correlation of natural killer cell activity and clearance of *Cryptococcus neoformans* from mice after adoptive transfer of splenic nylon wool nonadherent cells. Infect. Immun. **51**:547–555.
11. **Hidore, M. R., and J. W. Murphy.** 1987. Natural cellular resistance of beige mice against *Cryptococcus neoformans*. J. Immunol. **137**:3624–3631.
12. **Hidore, M. R., and J. W. Murphy.** 1989. Murine natural killer cell interactions with a fungal target, *Cryptococcus neoformans*. Infect. Immun. **57**:1990–1997.
13. **Hidore, M. R., N. Nabavi, C. W. Reynolds, P. A. Henkart, and J. W. Murphy.** 1990. Cytoplasmic components of natural killer cells inhibit the growth of *Cryptococcus neoformans*. J. Leukocyte Biol. **48**:15–26.
14. **Hiserodt, J. C., and T. F. Beals.** 1985. Ultrastructural analysis of human natural killer cell-target cell interactions leading to target cell lysis, p. 195–204. *In* R. B. Herberman and D. M. Callewaert (ed.), Mechanisms of cytotoxicity by NK cells. Academic Press, Orlando, Fla.
15. **Hiserodt, J. C., L. J. Britvan, and S. R. Targen.** 1982. Characterization of the cytolytic reaction mechanism of the human natural killer (NK) lymphocyte: resolution of binding, programming, and killer cell-independent steps. J. Immunol. **129**:1782–1787.
16. **Hiserodt, J. C., L. J. Britvan, and S. R. Targan.** 1982. Differential effects of various pharmacologic agents on the cytolytic reaction mechanism of the human natural killer lymphocyte: further resolution of programming for lysis and KCIL into discrete stages. J. Immunol. **129**:2266–2270.
17. **Huwyler, T., A. Hirt, D. Felix, and A. Morell.** 1985. Effect of cations and cation channel blockers on human natural killer cells. Int. J. Immunopharmacol. **7**:573–576.
18. **Julius, M. H., E. Simpson, and L. A. Herzenberg.** 1973. A rapid method for isolation of functional thymus-derived lymphocytes. Eur. J. Immunol. **3**:645–649.
19. **Katz, P., A. M. Zaytoun, and J. H. Lee, Jr.** 1982. Mechanisms of human cell-mediated cytotoxicity. III. Dependence of natural killing on microtubule and microfilament integrity. J. Immunol. **129**:2816–2825.
20. **Kiessling, R. E., E. Klein, and W. Wigzell.** 1975. "Natural" killer cells in the mouse. I. Cytotoxic cells with specificity for mouse Moloney leukemia cells. Specificity and distribution according to phenotype. Eur. J. Immunol. **5**:112–117.
21. **Kupfer, A., G. Dennert, and S. J. Singer.** 1983. Polarization of the Golgi apparatus and microtubule-organizing center within cloned natural killer cells bound to their targets. Proc. Natl. Acad. Sci. USA **80**:7224–7228.
22. **Kupfer, A., G. Dennert, and S. J. Singer.** 1985. The reorientation of the Golgi apparatus and the microtubule-organizing center in the cytotoxic effector cell is a prerequisite in the lysis of bound target cells. J. Mol. Cell. Immunol. **2**:37–49.
23. **Kupfer, A., and S. J. Singer.** 1989. Cell biology of cytotoxic and helper T cell functions: immunofluorescence microscopic studies of single cells and cell couples. Annu. Rev. Immunol. **7**:309–337.
24. **Luini, W., D. Baraschi, S. Alberti, A. Aleotti, and A. Tagliabue.** 1981. Morphological characterization of a cell population re-

sponsible for natural killer activity. Immunology **43**:663–668.
25. **Millard, R. W., D. A. Lathrop, G. Grupp, M. Ashraf, I. L. Grupp, and A. Schwartz.** 1982. Differential cardiovascular effects of calcium channel blocking agents: potential mechanisms. Am. J. Cardiol. **49**:499–506.
26. **Murphy, J. W.** 1989. Natural host resistance mechanisms against systemic mycotic agents, p. 149–184. *In* C. W. Reynolds and R. H. Wiltrout (ed.), Functions of the natural immune system. Plenum Publishing Corp., New York.
27. **Murphy, J. W., and G. C. Cozad.** 1972. Immunological unresponsiveness induced by cryptococcal capsular polysaccharide assayed by the hemolytic plaque technique. Infect. Immun. **5**:896–901.
28. **Murphy, J. W., and D. O. McDaniel.** 1982. In vitro reactivity of natural killer (NK) cells against *Cryptococcus neoformans*. J. Immunol. **128**:1577–1583.
29. **Nabavi, N., and J. W. Murphy.** 1985. In vitro binding of natural killer to *Cryptococcus neoformans* targets. Infect. Immun. **50**:50–57.
30. **Podack, E. R.** 1988. Granule-mediated cytolysis of target cells. Curr. Top. Microbiol. Immunol. **140**:1–9.
31. **Reynolds, E.** 1963. The use of lead at a high pH as an electron-opaque stain in electron microscopy. J. Cell Biol. **17**:208–213.
32. **Roder, J. C., R. Kiessling, P. Biberfeld, and B. Andersson.** 1978. Target-effector interaction in the natural killer (NK) cell system. J. Immunol. **121**:2509–2517.
33. **Rogers, K. A., M. A. Khoshbaf, and D. L. Brown.** 1981. Relationship of microtubule organization in lymphocytes to the capping of immunoglobulin. Eur. J. Cell Biol. **24**:1–8.
34. **Ryser, J., E. Rungger-Brandle, C. Chaponnier, G. Gabbiani, and P. Vassalli.** 1982. The area of attachment of cytotoxic T lymphocytes to their target cells shows high motility and polarization of actin, but not myosin. J. Immunol. **128**:1159–1162.
35. **Sirianni, M. C., S. Soddus, W. Malorni, G. Arancia, and F. Aiuti.** 1988. Mechanism of defective natural killer cell activity in patients with AIDS is associated with defective distribution of tubulin. J. Immunol. **140**:2565–2568.
36. **Solovera, J. J., M. Alvarez-Mon, J. Casas, J. Carballido, and A. Dutantez.** 1987. Inhibition of human natural killer (NK) activity by calcium channel modulators and a calmodulin antagonist. J. Immunol. **139**:876–880.
37. **Spurr, A. R.** 1969. A low-viscosity epoxy resin embedding medium for electron microscopy. J. Ultrastruct. Res. **26**:31–43.
38. **Targen, S. R., and R. L. Deem.** 1985. NK-target cell interactions in binding, triggering, programming, and lethal hit of NK cytotoxicity, p. 155–172. *In* R. B. Herberman and D. M. Callewaert (ed.), Mechanisms of cytotoxicity by NK cells. Academic Press, Orlando, Fla.
39. **Ullberg, M., and M. Jondal.** 1981. Recycling and target binding capacity of human killer cells. J. Exp. Med. **153**:615–628.